

Runaway Electron Dynamics and Critical Electric Field for Runaway Generation in the FTU Tokamak

Z. Popovic ¹, B. Esposito ², J. R. Martin-Solis ¹, W. Bin ³, L. Boncagni ²,
D. Carnevale ⁴, M. Gospodarczyk ⁴, D. Marocco ², G. Ramogida ² and M. Riva ²

¹ Universidad Carlos III de Madrid, Avda. Universidad 30, 28911-Madrid, Spain.

² ENEA for EUROfusion, via E. Fermi 45, 00044 Frascati (Roma), Italy.

³ Istituto di Fisica del Plasma - CNR, Via R. Cozzi 53, 20125 Milano, Italy.

⁴ Dip. di Ingegneria Civile ed Informatica DICII, Universita di Roma, Tor Vergata, Via del Politecnico 1, 00133 Roma, Italy.

1. Introduction Large amounts of MeV runaway electrons (REs) generated during disruptions pose a significant danger for the operation of next-step devices like ITER. RE suppression by Massive Gas Injection (MGI) relies on increasing the electron density (and, hence, the electric field) above their critical values where no REs can be generated. Here, we report on experiments designed to evaluate the threshold electric field for runaway generation during the flat-top of ohmic (OH) discharges in the FTU tokamak. The measured threshold electric field is found to be significantly larger ($\sim 2 - 5$ times) than predicted by the classical collisional theory and can be explained to a great extent by the electron synchrotron radiation losses. Simulations of the RE dynamics (generation and energy evolution) during these experiments will be also presented.

2. Experiments and data analysis The relativistic collisional theory predicts that for runaway creation a threshold electric field $E_R = n_e e^3 \ln \Lambda / (4\pi \epsilon_0^2 m_e c^2)$ should be exceeded. In FTU, the results have been consistent with an increase of E_R due to the electron synchrotron radiation losses [1]:

$$\frac{E_R^{rad}}{E_R} \cong 1 + C(Z_{eff}) F_{gy}^\alpha,$$

where $\alpha = 0.45 \pm 0.03$, $F_{gy} \equiv 2\epsilon_0 B_0^2 / (3n_e \ln \Lambda m_e)$, $C(Z_{eff}) \cong 1.64 + 0.53 Z_{eff} - 0.015 Z_{eff}^2$.

Here, the critical conditions have been tested during the flat-top phase of OH discharges in two experimental scenarios, as illustrated in Fig. 1: RE *onset* experiments (left, Fig. 1) in which the density is decreased until REs are generated and RE *suppression* (right, Fig. 1) of existing REs (created during a low density start-up) by gas injection. The presence of the REs is detected by the divergence of the BF₃ neutron detector and the NE213 neutron/gamma scintillator signals which allow to determine the critical time t_c at which the REs appear/disappear in the onset/suppression experiments [2]. The threshold field is estimated as $E_{thr} \sim V_{loop}(t_c) / 2\pi R_0$.

The database of analysed discharges covers a wide range of plasma parameters ($B_t = 2 - 7.2$ T, $I_p = 0.35 - 0.9$ MA and $Z_{eff} = 1.5 - 10$). The results (Fig. 2) are consistent with previous findings [1]: E_{thr} is several times ($\sim 2 - 5$) larger than the relativistic

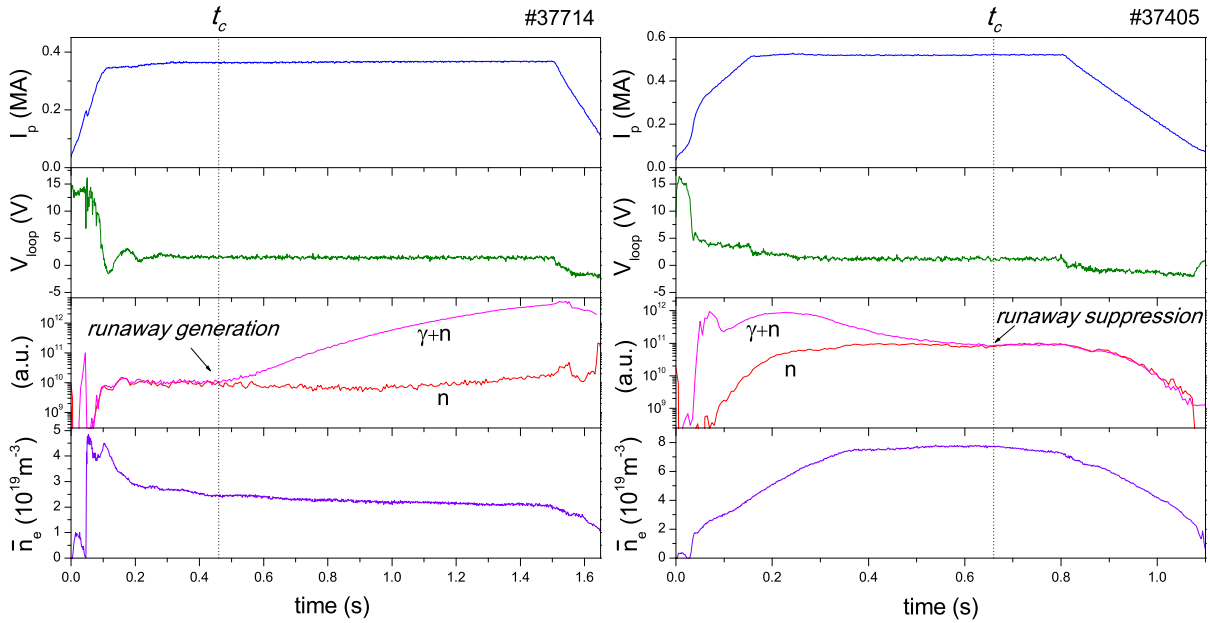


Figure 1: Time traces of the plasma current (I_p), loop voltage (V_{loop}), NE213 ($\gamma+n$) and BF_3 (n) signals and line-averaged central density for representative discharges: RE onset (left) and RE suppression (right).

collisional theory predictions, E_R (Fig.2, left) and falls well within the range of critical fields predicted including the effect of the electron synchrotron radiation losses, E_R^{rad} (Fig. 2, right). The local central density is used to calculate E_R and E_R^{rad} since REs are observed to be mostly generated in the centre of the plasma [1]. These findings are in agreement with a recent ITPA joint experiment in several tokamaks [3] and suggest that REs might be suppressed at lower densities than expected which could have important implications for RE mitigation in ITER.

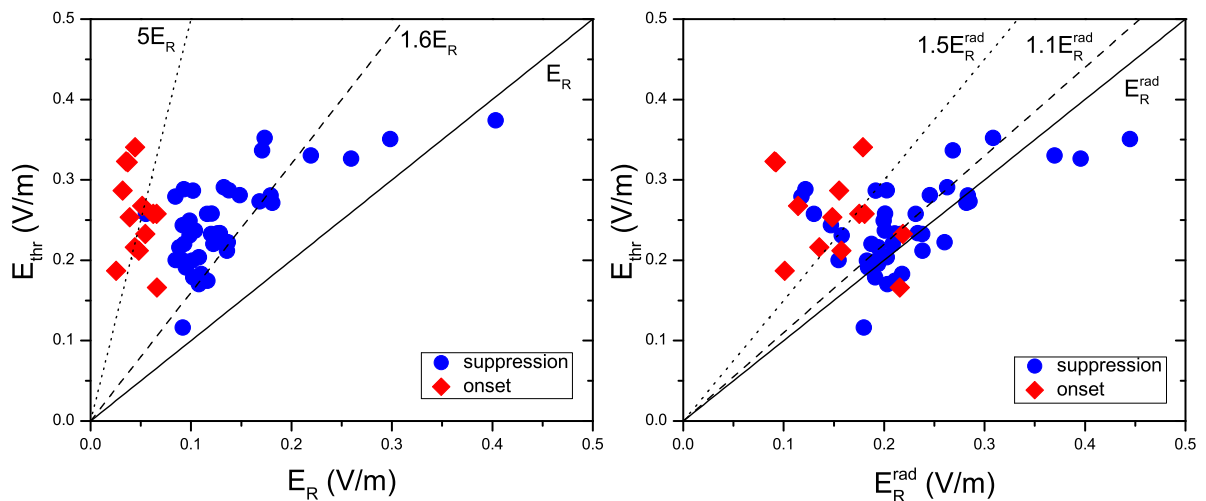


Figure 2: Comparison of E_{thr} with the relativistic collisional theory, E_R , (left) and synchrotron radiation theory E_R^{rad} (right). Each point corresponds to a single discharge.

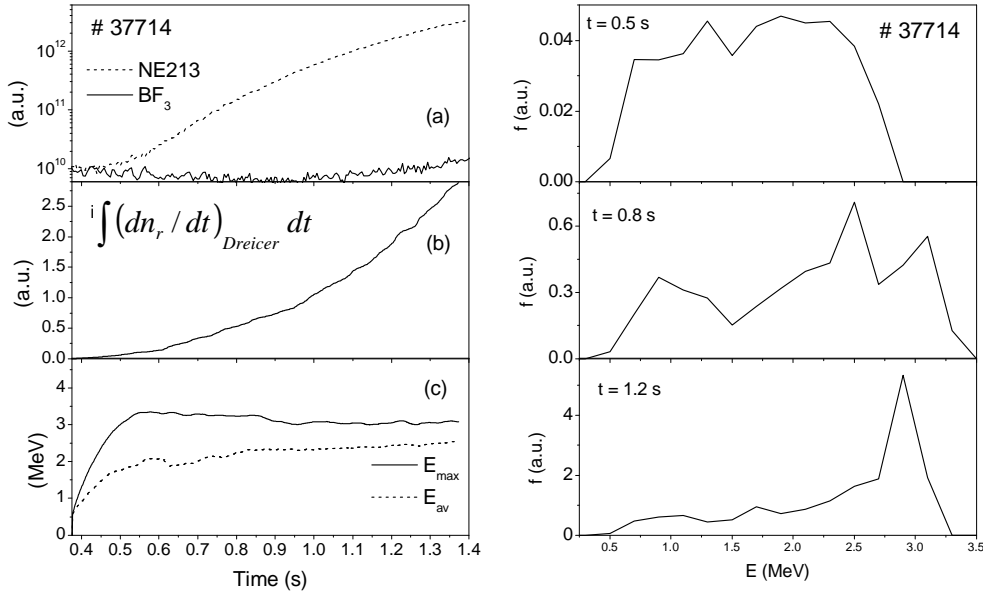


Figure 3: For RE onset discharge # 37714: **Left:** Time evolution of BF_3 and $NE213$ scintillator signals (a), estimated runaway production (b), maximum and average runaway energies (c); **Right:** Calculated runaway distribution function at 0.5, 0.8 and 1.2 s.

3. Runaway Dynamics The runaway dynamics for the RE onset and suppression experiments of Fig. 1 is illustrated in Figs. 3 and 4, respectively. For the case of the RE onset discharge (Fig. 3), the runaway production [trace (b)], calculated assuming to be dominated by the Dreicer mechanism, as typically observed in FTU OH discharges [3], is qualitatively consistent with the runaway measurements [traces picture (a)]. The runaway energy distribution function, $f(E)$, has been estimated calculating the energy evolution of the generated runaway electrons by means of a simple test particle model for the runaway dynamics [4] including the electric field acceleration, collisions with the plasma particles and deceleration due to synchrotron radiation losses. Then, the runaway distribution function is formally given by:

$$f(E, t) = \int_0^t \frac{dn_r}{dt'} (E_0, t') dt', \quad (1)$$

where $t = 0$ denotes the start of the runaway generation and the integration is carried out over the times t' for which an electron generated with energy E_0 would have gained, according to the test particle equations, an energy E at time t . The resulting distribution function at three different times during the discharge is plotted in right Fig. 3, whereas the time evolution of the maximum and average electron energies (E_{max} and E_{av}) is plotted in Fig. 3 (c). The distribution function is broad, extending up to the maximum runaway energy at each time step, and showing a trend along the discharge to accumulate close to the limiting energy ~ 3 MeV.

The RE suppression experiment is presented in Fig. 4. REs are generated in the beginning of the discharge (due to the large electric field and low density, Fig. 1) and the runaway production stops soon during the current ramp-up at ~ 0.15 s [trace (b)].

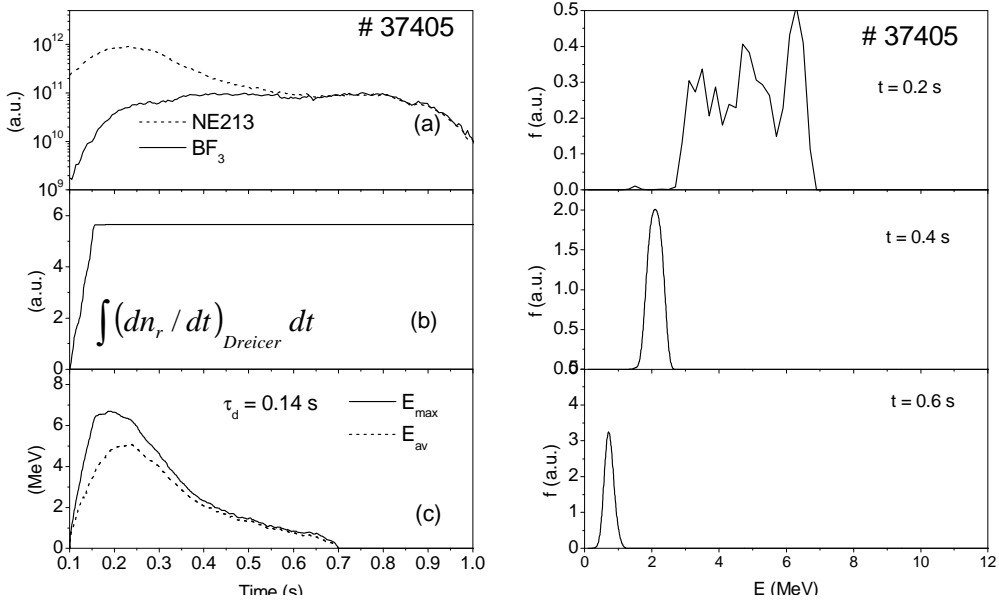


Figure 4: For RE suppression discharge # 37405: **Left:** Time evolution of BF_3 and $NE213$ scintillator signals (a), estimated runaway production (b), maximum and average runaway energies (c); **Right:** Calculated distribution function at 0.2, 0.4 and 0.6 s.

The runaway energy increases up to ~ 7 MeV [trace (c)] and decreases later on along the discharge until the REs are suppressed. As the runaway production stops early in the discharge (~ 0.15 s), the distribution function, initially broad ($t = 0.2$ s in right figure), evolves towards a mono-energetic runaway beam ($t = 0.4$ and 0.6 s in right Fig.4) with an average energy equal to the maximum runaway energy [Fig.4 (c)]. For most of the analysed RE suppression discharges, the electron radiation cannot account for all the runaway losses (typically $E_{\text{thr}} > E_R^{\text{rad}}$, as shown in Fig. 2) and additional energy dissipation mechanisms must be invoked to explain the observed RE suppression (in Fig. 4, a characteristic dissipation time $\tau_d \sim 0.14$ s has been assumed in the simulations to describe such unknown processes).

Acknowledgements

This work was done under financial support from Dirección General de Investigación, Científica y Técnica, Project No.ENE2012-31753 and within the framework of the EUROfusion Consortium and has received funding from the Euratom research and training programme 2014-2018 under grant agreement No 633053. The views and opinions expressed herein do not necessarily reflect those of the European Commission.

References

- [1] B. Esposito et al., in Fusion Energy 2014 (Proc. 25th Int. Conf., St. Petersburg, 2014) (Vienna: IAEA) CD-ROM file EX/P2-50.
- [2] B. Esposito et al., Phys. Plasmas **10** (2003) 2350.
- [3] R. Granetz et al., Phys. Plasmas **21** (2014) 072506.
- [4] J.R. Martin-Solis et al., Phys. Plasmas **5** (1998) 2370.